Atomic-Scale Insights into Hydrodesulfurization†

J. G. Kushmerick,‡ S. A. Kandel, P. Han, J. A. Johnson,§ and P. S. Weiss*

Department of Chemistry, The Pennsylvania State University, University Park, Pennsylvania 16802-6300

Received: September 16, 1999; In Final Form: January 24, 2000

We have used low-temperature ultrahigh vacuum scanning tunneling microscopy to gain atomic-scale insights into the hydrodesulfurization process. Investigations of Ni adsorbed on the basal plane of MoS_2 revealed that the Ni adatoms are highly mobile due to their weak interaction with the exposed sulfur atoms. The Ni adatoms rapidly diffuse about the surface down to 77 K, and even at 4 K are easily manipulated with the STM probe tip. Spectroscopic imaging of Ni clusters adsorbed on the MoS_2 basal plane reveals that their electronic structure is well suited to bind nucleophilic reactant species. From low-temperature STM images of thiophene adsorbed on Ni{110}, a bonding geometry is proposed. New roles for metal promoter atoms in hydrodesulfurization catalysis, based on these results, are suggested.

1. Introduction

Hydrodesulfurization Catalysis. Nickel (Ni)- or cobalt (Co)-promoted molybdenum disulfide (MoS_2) hydrodesulfurization (HDS) catalysis is one of the most widely used catalytic systems worldwide.[1] HDS removes sulfur from petroleum feedstock in order to avoid sulfur poisoning of Pt-based reforming catalysts as well as to make the end petroleum products more environmentally friendly. President Clinton in a speech on May 1, 1999 announced a new Environmental Protection Agency regulation calling for a 90% reduction of sulfur content in automobile gasoline in the United States by the year 2004. Similar efforts are underway around the world. Because of its enormous industrial and environmental importance, many approaches have been taken to attempt to understand this catalytic system. These research investigations have utilized the techniques of surface science,[2] heterogeneous catalysis,[3] organometallic chemistry,[4] and theoretical chemistry.[5]

The industrial catalysts typically consist of MoS_2 crystallites on alumina supports promoted with Ni or Co. It has been well established that the activity and selectivity of the catalysts stem from the MoS_2 phase and that the alumina primarily acts to disperse and to stabilize the MoS_2 domains.[3] Most studies attempt to elucidate the chemical function of the catalyst either from direct measurements of small batch reactors or from investigations of model systems. Many of these model systems employ MoS_2 single crystals, which are particularly amenable to investigation by standard surface-science techniques. In this paper, we present data from two model systems relevant in the study of HDS: we report observations of nickel atoms and clusters on a MoS_2 single-crystal surface, as well as measurements of thiophene (C_4H_4S) on single-crystal Ni{110}.

MoS_2 has a layered crystal structure consisting of sheets of S−Mo−S, with these sheets weakly bound to each other by van der Waals interactions. This leads to relatively inert basal planes with unsaturated (presumably reactive) exposed plane edges. Some of the earliest attempts to understand HDS have taken into account this heterogeneous structure.[6]

Thiophene and its derivatives are studied as model reactants for HDS since they represent the most difficult compounds in fuel feedstocks to desulfurize.[7] Salmeron et al. deduced that the MoS_2 basal planes are inert and show negligible activity for thiophene HDS.[8] Upon sputtering of the MoS_2 basal plane the thiophene HDS activity increased, consistent with the hypothesis that exposed Mo atoms at sheet edges are the active site for HDS.[9] Applying a concert of surface science techniques to determine the activity of these MoS_2 edge sites proved to be difficult, as a result of the difficulty of forming well-ordered stepped surfaces. Single-crystal Mo surfaces bare and with adsorbed S have been studied as model systems.[10] The Mo single crystals have significantly different structures and higher reactivity than MoS_2, which can make it difficult to extrapolate to the industrially relevant catalysts. Recently, nanocrystalline platelets of metal sulfides have been grown on metal substrates so that their chemical and electronic properties could be probed.[11,12]

The MoS_2 dispersion (the ratio of edge to basal plane sites) plays an important role in determining the activity of the catalyst. An interesting study that measured the catalytic activity as a function of the MoS_2 crystal morphology suggests that the presence of basal plane affects the catalytic activity.[13] Daage and Chianelli modified the morphology of an unsupported MoS_2 catalyst by treating it with O_2 or HCl.[13] The resulting surface had the same number of equivalent step edge sites (and thus active sites for HDS) yet the step edges were more likely to have adjacent basal planes after the roughening treatment. Daage and Chianelli found that the selectivity for hydrogenation vs HDS depends on the local environment of the edge site. Edge planes that are sandwiched between other edge planes have a higher probability to perform HDS while edge sites that have surrounding basal plane perform more hydrogenation. More importantly for the studies described below, they also noted that the catalytic activity increased when the stacking pattern went from predominantly sandwiched edge sites to edge sites surrounded by basal plane.[3,13] These studies demonstrate that while basal planes are unreactive by themselves, they still play an important role in the catalytic system.

† Part of the special issue "Gabor Somorjai Festschrift".

* Corresponding author. E-mail: stm@psu.edu. Fax: 1-814-863-5516.

‡ Present address: Biomolecular Materials and Interfaces, Sandia National Laboratories, Albuquerque, NM 87185.

§ Present address: Commonwealth Governor's School, Fredericksburg, VA 22405.

10.1021/jp993319i CCC: $19.00
Published on Web 03/21/2000

Promoter Effect. The structure and bonding of the metal promoter atoms have been investigated extensively in situ with Mössbauer emission spectroscopy and extended X-ray absorption fine structure (EXAFS). Topsøe and co-workers have shown that promoter atoms are primarily located at MoS_2 sheet edges in the form of Ni(Co)−Mo−S structures.[14−16] These structures are now believed to dominate the catalytic reactivity of the system.[17] In the preparation of the catalysts, the conditions are set such that Mo is sulfided while the promoters are not.

A number of hypotheses exist for the roles of the catalytic promoters (Ni and Co) in MoS_2-based HDS catalysts, and a review of HDS promoters is presented by Somorjai and co-workers in ref 18. Two of these hypotheses are consistent with the structure and activity observations of Topsøe and co-workers. The first model proposes that promoter atoms increase the electron density on the Mo atoms and that these reduced Mo atoms have enhanced HDS activity.[19] The second model suggests that the promoter atoms actually create new catalytic sites and thus might more rightfully be considered a part of the catalytic phase instead of a promoter.[20] The apparent advantage of keeping the promoters unsulfided was put forward as supporting this latter model since these promoter atoms were expected to decorate the crystallite edge sites.

The main difficulty in differentiating between these two models is the inability to monitor directly in real space the catalytically active surface structures of such a system. Scanning tunneling microscopy can overcome some of the limitations that other techniques have in studying MoS_2 as a model of the HDS catalytic system. Specifically, since measurements of single nanometer-scale structures are routine, it is not necessary to prepare a well-ordered array of surface structures, such as those needed for optical or thermal techniques, which measure ensemble averages of surface properties. On the other hand, it can be difficult to show that the structures observed are typical and/or relevant.

On the basis of our observation that Ni atoms remain mobile on the MoS_2 basal plane even at reduced temperature (77 K), we proposed two additional roles for promoters.[21] First, mobile promoters would have the effect of enhancing sticking of the reactants and intermediates on the basal plane. This would result from the formation of an inorganic complex between the promoter atom(s) and the molecule. Second, this complex would be mobile and thus would give the molecules the means to transit the surface to sample different potential sites for reaction. This sticking and subsequent mobility would greatly enhance the reactivity of the catalyst.[21] These mechanisms are also consistent with the prior observations of structures, preparation, and activity of the catalysts.

Scanning Tunneling Microscopy of MoS_2. MoS_2 and the other transition-metal dichalcogenides have been studied extensively by STM, as they cleave easily to form atomically flat surfaces suitable for STM imaging.[22−28] Magonov and Whangbo argued that since the d orbitals fall off much more rapidly in space than s and p orbitals, it is the S atoms that are imaged.[23] Weimer et al. reported simultaneous observation of both the S and Mo atoms in their STM study.[24] Sautet and co-workers suggested that at large tip−sample separations, protrusions in constant current STM images correspond to the surface sulfur atoms, while at smaller separations both the S and Mo atoms are imaged.[29]

The nature of STM images of defect structures on MoS_2 has also been studied.[30] Peculiar ring structures observed on naturally occurring MoS_2 crystals have been attributed to intercalation of impurity atoms or molecules during crystal formation.[31,32] Permana et al. attribute the observed ring structures to electronic effects from vanadium and fluoride ion impurities intercalated in the Mo layer of MoS_2.[32] Heckl et al. give the more provocative and speculative assignment of trapped biological material included during the hydrothermal formation of natural MoS_2 (molybdenite).[31]

Chu and Schmidt used AFM and STM to monitor the gasification of MoS_2 by H_2, demonstrating the applicability of scanning probe techniques to investigations of MoS_2-based HDS catalysis.[33] Chu and Schmidt found that upon heating the $MoS_2\{0001\}$ surface in H_2 two processes occurred: first, the top surface sulfur layer was removed from around defects and pits, and second, the newly exposed Mo layer formed into clusters, which further accelerated the removal of the S layer. Addition of thiophene to the H_2 gas was found to retard the S gasification and thus it was suggested that the exposed Mo atoms are active sites for HDS. The roles of promoter atoms in gasification were also studied, and it was shown that Ni and Co catalyze the gasification of the MoS_2 surface and greatly increase the total number of edge sites.

Thiophenes on Metal Surfaces. Thiophene and its derivatives form transition-metal complexes by coordinating through either their p electrons (η^5 bonding) or the S atom's lone pair of electrons (η^1 bonding).[34] No prior experimental results for thiophene adsorption on Ni{110} could be found in the literature. Zaera et al. and Huntley et al. used high-resolution electron energy loss spectroscopy to probe the adsorption geometry of thiophene on Ni{100},[35] and Ni{111},[36] respectively. Both studies revealed that thiophene binds to the Ni surface through the S atom (η^1 bonding); however, some rehybridization of the S atom may occur (sp^2 to sp^3) causing the molecular adsorbate to be tilted with respect to the surface normal. Thus, a similar η^1 bonding for thiophene on Ni{110} appears to be reasonable.

Hamers and co-workers imaged rotational orientation of thiophene derivatives on a Ag{111} surface.[37] Hamers and co-workers also investigated the contrast mechanism for these molecules in an attempt to assign molecular orientation unambiguously.[37] Chen et al. proposed that the rotational orientation of dimethylthiophene at Ag(111) step edges is due to a combination of molecule-substrate interactions and intermolecular dipole−dipole interactions.[38]

2. Experimental Section

Crystal Structures. Because of the S−Mo−S sheet stacking in MoS_2, cleaving the crystal to reveal the $MoS_2(0001)$ surface or basal plane always results in the exposure of a sulfur-terminated surface. These exposed sulfur atoms have saturated bonding within the sheets and thus are extremely unreactive.[8,9]

The Ni(110) surface has rectangular symmetry with close-packed rows of Ni atoms with a spacing of 2.45 Å along the $[\bar{1}10]$ direction and an interrow spacing of 3.46 Å in the [001] direction.

Instrumentation. All experiments were performed in a stainless steel UHV system described in detail in ref 39, equipped with low-energy electron diffraction (LEED), Auger electron spectroscopy (AES), and low-temperature STM capabilities. Briefly, three room-temperature UHV chambers contain the surface preparation and analysis tools. A VG Microtech RVL 900 capable of both LEED and AES is mounted in the surface preparation chamber.[40] A connected low-temperature stage contains the home-built beetle-style STM, with multiple layers of vibration isolation separating the microscope from the

surrounding environment. The STM can be operated at room temperature, 77 K, or 4 K. The base pressure of the UHV system at room temperature is in the 10^{-11} Torr range and goes down with reducing temperature to the 10^{-14} Torr range.

Sample Preparation. Natural MoS_2 single crystals, molybdenite, were used in this study.[41] The samples were cleaved in air using adhesive tape prior to insertion into the UHV chamber. The cleaving process removes the top few layers of MoS_2 leaving a single-crystal surface suitable for investigation. After mounting, the samples were annealed to 600 °C in UHV to remove surface contaminants. The LEED pattern of samples prepared this way shows the (1 × 1) hexagonal pattern consistent with the idealized termination of the bulk crystal structure. To check the surface composition of our samples, AES was performed; no peaks other than Mo and S are visible in the Auger spectra.

Ni was deposited onto a room temperature MoS_2 surface by sublimation of a 1.0 mm diameter 99.99+% Ni wire in UHV. An exposure of 6×10^{-8} Torr s yielded a dilute coverage of ~6%, suggesting a sticking coefficient near unity. The MoS_2 sample was then transferred (within UHV) to the STM maintained at 298, 77, or 4 K.

The Ni{110} crystal was prepared by repeated cycles of 1 keV Ar^+ sputtering and 925 K anneal cycles. O_2(g) reaction cycles removed the residual surface carbon contamination. Despite these procedures, some surface S contamination persisted. Adsorbed S atoms are apparent in the STM images (see below).

Thiophene obtained from Aldrich (99%) was purified by repeated freeze−pump−thaw cycles. The purity of the thiophene was determined in situ with mass spectrometry. Thiophene was dosed onto the Ni{110} crystal by back-filling the room temperature UHV chamber through a sapphire leak valve and then rotating the crystal, at the low-temperature stage, to allow controlled exposure. The dosing procedure is described in more detail in ref 39.

3. Results and Analysis

Clean MoS_2. Atomic resolution images of the clean MoS_2 surface exhibit the hexagonal symmetry and 3.2 Å lattice constant of the exposed sulfur atoms of the basal plane (see Figure 1 of ref 21). The tunneling conditions used for imaging in this study are such that the STM tip was far from the surface and thus protrusions are attributed to the surface sulfur atoms.[29]

While the vast majority of the surface imaged showed only flat terraces, a few defect structures were also found on the surface. Ring structures similar to those previously reported were observed.[31,32] These ring structures are imaged as apparent protrusions from the MoS_2 surface with diameters of 50−100 Å. Figure 1A is an STM image of two adjacent ring structures. As mentioned above, these ring structures have been attributed to impurities trapped between MoS_2 layers during formation, and not to surface species.[32] Figure 1B is a high-resolution image of the edge of the larger ring shown in Figure 1A. The atomic lattice is visible both around and inside the ring. Areas with such large scale defects were deliberately avoided when studying Ni adsorbed on MoS_2.

Ni on MoS_2: Dynamics. After depositing Ni adatoms on the sample, STM imaging showed that Ni atoms diffuse rapidly on the basal plane of MoS_2. Diffusion of adsorbed Ni atoms prevented acquisition of stable images at 298 and 77 K. The Ni species diffused across the surface on a submillisecond time scale inaccessible to imaging with our STM[42] and thus the images were dominated by apparent current noise as atoms moved rapidly on the surface through the tunnel junction.[43−45]

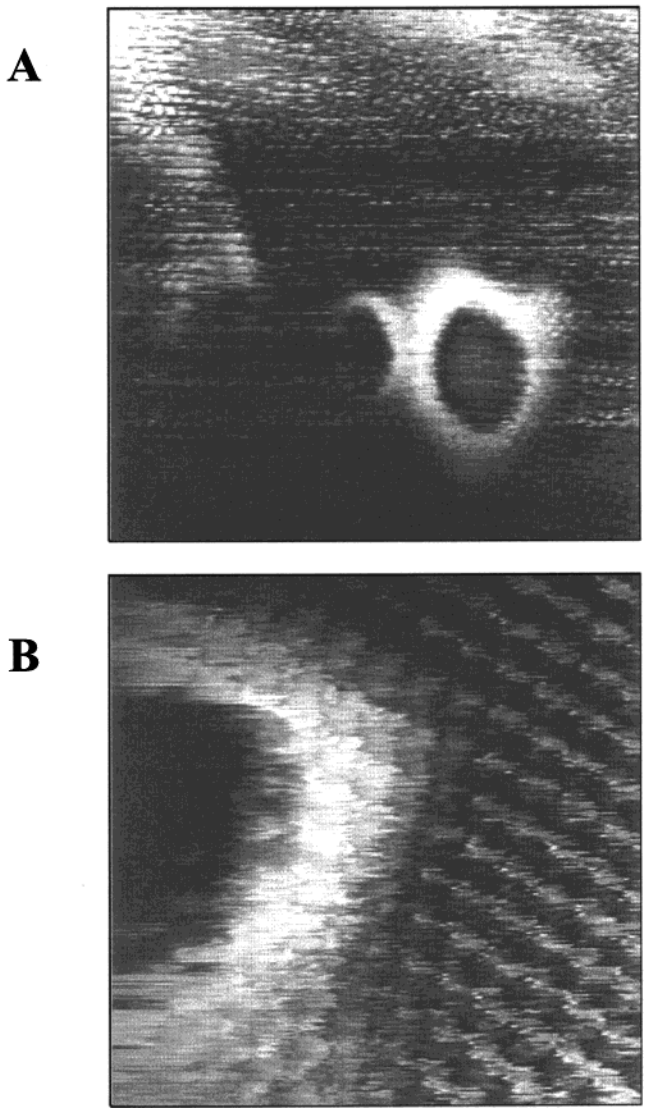

Figure 1. (A) STM image of two ring structures on MoS_2 basal plane (200 Å × 200 Å image area, sample bias = −500 mV, tunneling current = 200 pA, temperature = 77 K). (B) STM image of the edge of one ring structure. Atomic resolution of MoS_2 basal plane is apparent, even within the ring (50 Å × 50 Å image area, sample bias = −500 mV, tunneling current = 200 pA, temperature = 77 K).

At 4 K, isolated atoms and small clusters of Ni are stable and can be imaged. Even at 4 K, single Ni atoms can be easily manipulated with the microscope tip. By lowering the tunnel gap impedance the tip can be moved close enough to the surface to interact strongly with the Ni adsorbate and cause it to move across the surface with the STM tip.[46] Figure 2A is a representative image demonstrating tip-induced motion of a Ni adatom. The Ni atom is pulled from its adsorption site at a surface defect and dragged across the surface by the scanning tip. The Ni atom initially travels ca. 45 Å across the surface, then moves smaller amounts on each successive scan until it attaches to a preexisting cluster. Atomic clusters are more energetically stable and thus less affected by the microscope tip. This tip-assisted motion suggests the possibility of constructing large, well-defined clusters on the surface.[21]

Examining the initial 45 Å slide reveals that the tip-assisted diffusion is not a continuous motion but rather consists of the Ni atom making discrete hops between neighboring lattice

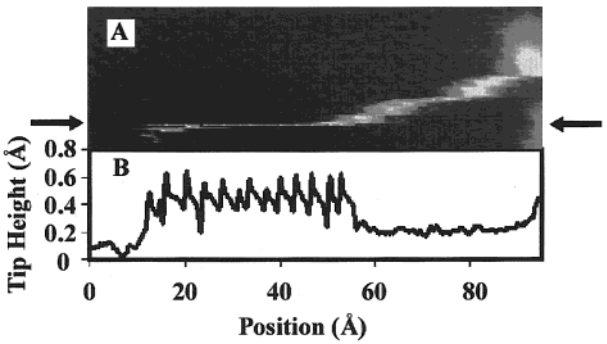

Figure 2. (A) An STM image showing the manipulation of a Ni adsorbate by the probe tip at 4 K (30 Å × 95 Å image area, sample bias = −1.5 V, tunneling current = 100 pA). Images are acquired line by line, from the bottom to the top as shown here. Data were collected as the tip moved from left to right in this image, then the tip was quickly moved back to the start of the next line. (B) Tip−sample separation during Ni motion is plotted. The line is indicated by the two arrows in Figure 2A. The motion of the tip indicates that the Ni adsorbate hops to neighboring lattice sites due to an attractive interaction with the STM probe tip.

sites.[47] The tip trajectory as the Ni atom is moved (determined by piezoelectric transducer motion under feedback control to maintain a constant tunneling current) is plotted in Figure 2B. This line is taken from the data shown in Figure 2A (between the points indicated by arrows). The STM probe tip initially approaches the Ni atom and retracts suddenly as the Ni atom hops from its adsorption site at a defect to under the tip. The tip then begins to scan down the contour of the Ni atom but retracts again when the Ni atom hops, one lattice site, back under the tip. This sequence of the STM tip scanning down the contour of the adatom only to retract suddenly when the Ni atom moves one lattice site under the tip is repeated for 45 Å, until the STM tip loses hold of the Ni adatom. Bartels et al. have shown that the shape of the tip motion can be used to determine the interaction between adsorbate and tip during lateral manipulation.[47] The tip trajectory observed in this case indicates that the Ni atom is being dragged by attractive interactions with the STM probe tip.

The distance between tip jumps, and thus Ni adsorption sites, is 3.3 Å, in good agreement with the lattice constant of 3.2 Å for this surface. The difference between the lattice constant of the surface and the jump separation actually may hold some insight into the reason that the tip loses "control" over the adatom. The fast scan direction for this image did not correspond with one of the six high-symmetry crystallographic directions. The Ni adatom follows the STM tip by jumping between equivalent adsorption sites along a particular lattice row. However, as a result of this mismatch, the Ni adatom must eventually jump between lattice rows in order to follow the tip over long distances, and this presumably increases the chance that the atom will "escape" from control of the tip.

Ni on MoS_2: Electronic Structure. Due to the high rate of diffusion for Ni adatoms on the $MoS_2\{0001\}$ surface it would be expected that after the initial deposition at room temperature the adatoms would be sufficiently mobile to "find" each other and nucleate into clusters if this were energetically favorable. Ni atoms and clusters are indeed found on the MoS_2 basal plane at 4 K. Ni clusters of various sizes from a few atoms to large islands were observed. Figure 3 is an image of a Ni_3 cluster on MoS_2.

Spectroscopic investigations of Ni clusters reveal the electronic origins for binding the S-containing nucleophilic molecules. Figure 4 shows the same Ni_3 cluster as in Figure 3

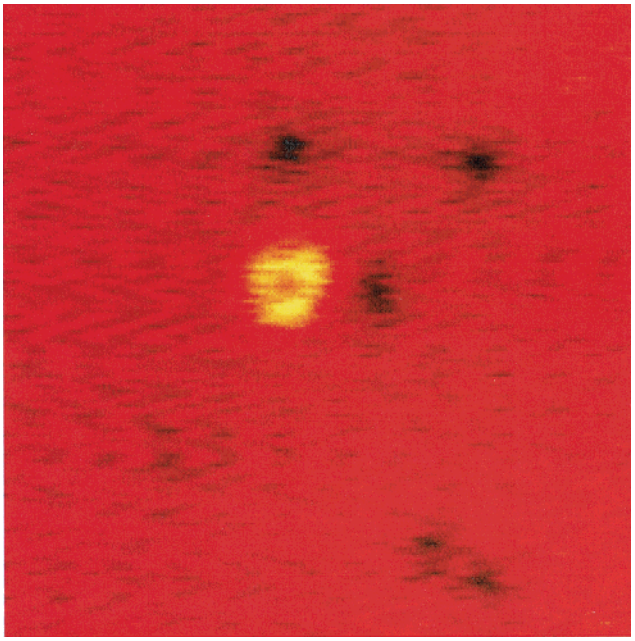

Figure 3. A Ni_3 cluster adsorbed on a MoS_2 basal plane at 4 K. Note the sulfur vacancies (appearing as dark spots) near the cluster as well as in the bottom right-hand corner. (100 Å × 100 Å image area, sample bias = +2 V, tunneling current = 100 pA, temperature = 4 K).

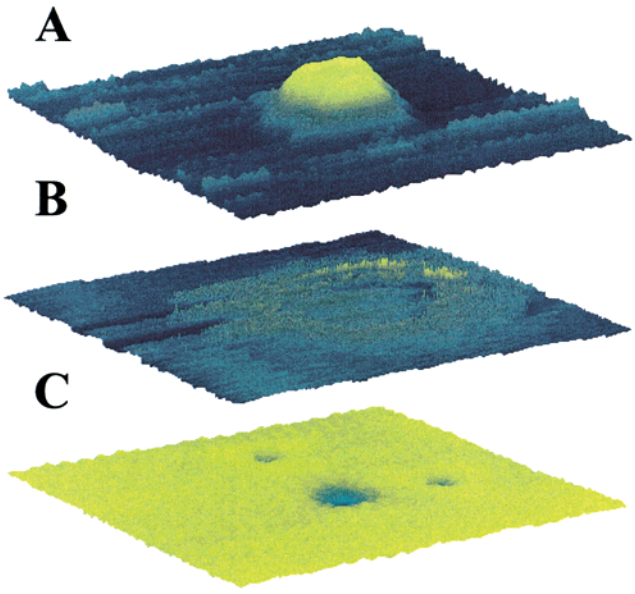

Figure 4. Three STM images of a Ni_3 cluster adsorbed on a MoS_2 basal plane at 4 K. All three images show a 60 Å × 60 Å area and are plotted as perspective views with the same aspect ratio and angle of view. The images were acquired with sample biases of +2 V (A), +1.4 V (B), and −2 V (C), and tunneling currents of 100, 100, and 200 pA, respectively. The Ni_3 cluster's effect on the local density of electronic states, both filled and empty, can be seen and is explained in the text.

imaged at three sample biases +2, +1.4, and −2 V from top to bottom, respectively. Imaging at these different bias voltages allows us to measure the effect the Ni cluster has on electronic states as a function of both position and energy.[48] At +2 V sample bias (electrons tunneling into the empty states on the surface), the Ni_3 cluster appears as a significant three-lobed protrusion from the MoS_2 basal plane (Figure 4A), indicating that the cluster increases the local density of empty electronic states at this energy. Likewise, we see from Figure 4C that the cluster depletes the density of filled states at 2 V below the

Fermi level (electrons tunneling from the filled sample electron states to the tip). The electronic structure observed is consistent with previous experimental results for Ni adsorption on MoS_2. Papageorgopoulos and Kamaratos found that charge transfer occurs when Ni is deposited on the basal plane of MoS_2.[49] From work function measurements they proposed that electron density from Ni is transferred to the p-band of the exposed S atoms.[49]

Such an electronic structure is well suited to bind nucleophilic (electron-rich) molecules or parts of molecules since there are empty orbitals to accept electron density, and depletion of filled orbitals repels an electron-rich molecule or moiety. The implications of this particular type of electronic structure are discussed below.

Two point defects in the MoS_2 surface are also found within this area (most apparent in Figures 3 and 4C). The point defects have previously been assigned as single S vacancies in the MoS_2 surface.[50] Such vacancies may stabilize the cluster and thus determine its position.[46c,51] Since we were unable to move this cluster with the STM probe tip, its binding site could not be determined,[46c] and thus whether it is sitting on the bare surface or has nucleated at a sulfur vacancy is unknown.

In the image acquired at a sample bias of +1.4 V the cluster is not apparent, but a diffuse ring ~30 Å in diameter surrounding it is found. This ring is well outside the geometric extent of the protrusion (~16 Å diameter), measured at +2 V sample bias. This ring results from a perturbation of the MoS_2 surface electronic structure by the Ni_3 cluster. This ring is substantially different from those observed around intercalation impurities mentioned above. Locally perturbed electronic structures by defects, steps, and adsorbates have been observed by STM to direct molecular adsorption,[44,45,52] affecting both adsorbate structures and chemistry. We have not yet observed such effects here but plan coadsorption studies to assess the importance of the local electronic effects on MoS_2 surface reactions.

Thiophene on Ni{110}. To gain understanding into the possible mechanism for thiophene binding to the Ni promoter species, adsorption of thiophene on Ni{110} was investigated. Prior to deposition of thiophene, the Ni{110} surface was imaged at 4 K to determine its crystallinity and defect density. Despite repeated attempts, we were unable to prepare a crystal completely free of S contamination as the S appears to be (and is typically) a bulk contaminant in Ni single crystals. All experimental results were thus acquired on a surface with a measurable amount of S contamination.

Figure 5 is an STM image of the Ni{110} surface after exposure to thiophene at 4 K. The thiophene molecules are clearly visible as protrusions on the Ni{110} terrace. The S contamination is also visible along with Ni−H added rows and one atom deep missing rows.[53] Figure 6 is a higher resolution image of thiophene on Ni{110}. The atomic rows along the $[\bar{1}10]$ direction are now visible. At this higher resolution the thiophene molecules appear to have an oval structure. The possibility of this structure being due to a tip artifact can be ruled out since two well-defined orientations for the thiophene molecules are observed. Thus, we attribute the features to the thiophene molecules. The shape of this feature is consistent with what one might expect for thiophene adsorbed normal to the Ni{110} surface.

Further examination of the STM images allows a tentative adsorption site assignment to be made. The thiophene molecules are centered between the rows of Ni atoms along the $[\bar{1}10]$ direction. This can be seen most clearly through a Fourier transform filtering technique. Figure 7 shows raw data and a Fourier transform filtered image of two thiophene molecules

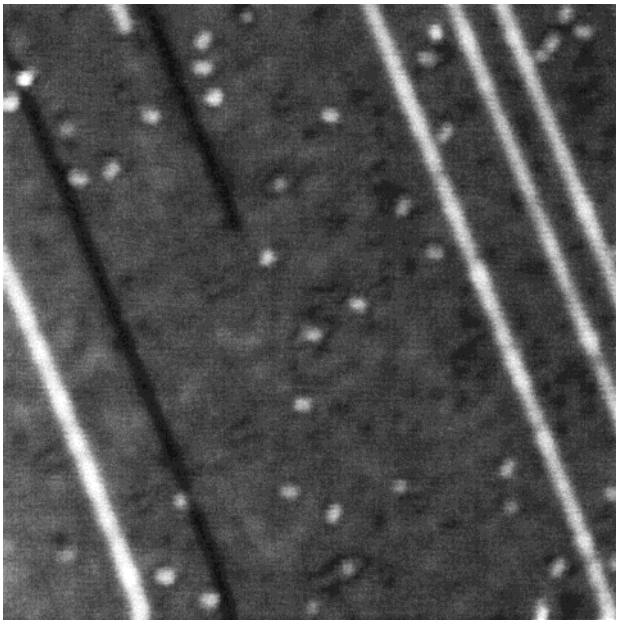

Figure 5. STM image of thiophene on Ni{110} at 4 K. The thiophene molecules are visible as protrusions on the Ni{110} terrace. Sulfur contaminants are visible as well as Ni−H added rows (white lines) and one atom deep missing rows (dark lines) (200 Å × 200 Å, sample bias = 50 mV, tunneling current = 1 nA).

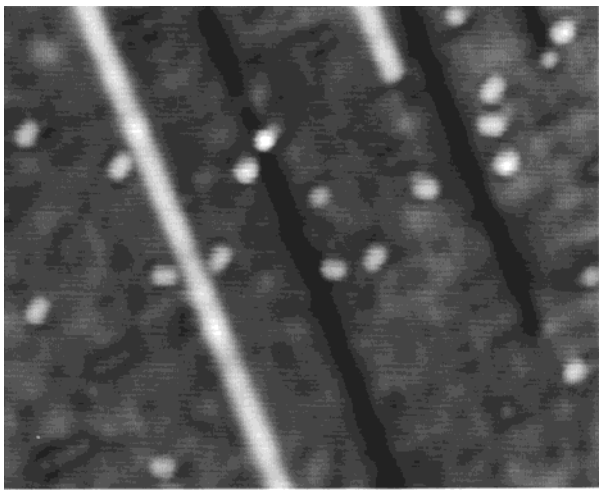

Figure 6. STM image of thiophene on Ni{110} at 4 K. The majority of thiophene molecules are imaged as oval spots with one of two distinct orientations (150 Å × 120 Å, sample bias = 50 mV, tunneling current = 1 nA).

on the Ni{110} surface.[54] The filtering technique consists of taking a two-dimensional Fourier transform of a selected part of the STM image and then reverse transforming only the spots corresponding to the Ni{110} lattice. This results in an image corresponding only to the substrate corrugation. The position of the thiophene molecules is then superimposed upon the filtered image to enable determination of the adsorption site.[55] This adsorption site assignment can also be made directly from our raw data; the Fourier filtering method facilitates the determination and the comparison of a number of data sets. Such a Fourier filtering technique was previously used to determine the adsorption sites of CO, C_2H_2, and C_2H_4 on Cu{110} and C_6H_6 on Cu{110} and Ni{110}.[56−58]

From the Fourier-filtered image it can be seen that thiophene sits between the closed-packed Ni atomic rows that lie along the $[\bar{1}10]$ direction. While it is not possible to determine directly from the filtered image whether thiophene adsorbs at the long

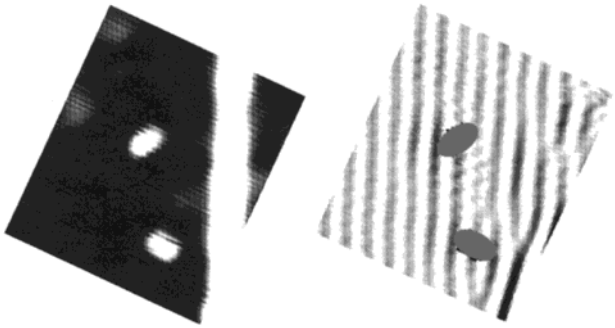

Figure 7. Raw data and Fourier transform filtered image of the Ni{110} surface with two thiophene adsorbates. The white line is a Ni−H added row. Both images were rotated to align the crystallographic directions with those of Figure 8. The filtering technique enhances the Ni atomic rows along the [110] direction. The adsorption site position of two thiophene molecules is superimposed upon the filtered image (40 Å × 45 Å, sample bias = 50 mV, tunneling current = 1 nA).

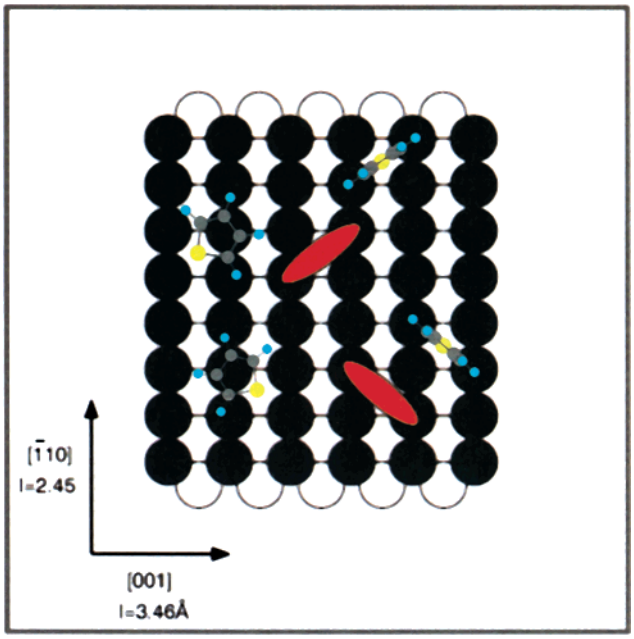

Figure 8. Schematic of the Ni{110} surface with the four high-symmetry adsorption sites labeled. The proposed adsorption sites for thiophene are indicated by the ovals. Note the two orientations are equivalent due to the symmetry of the crystal surface.

bridge site or the 4-fold hollow site, the angular orientations observed do suggest two possible adsorption geometries. In both proposed adsorption geometries the thiophene molecules are bound through their S atom at the 4-fold hollow site. The orientation of the molecular ring differs for the two possible geometries. In the first geometry the molecular plane is aligned with two of the Ni atoms constituting the "corners" of the 4-fold hollow site, thus maximizing its bonding interaction. In the second geometry the molecule is tilted and additionally bonds to a "corner" Ni atom through its delocalized p electrons. The observed oval features may then signify that the molecule were flipping between equivalent bonding environments with opposite "corner" atoms of the 4-fold hollow sites on a time scale inaccessible to our STM measurements. Adsorption of thiophene at the long bridge site can be ruled out for either bonding configuration proposed since the molecules would be aligned with atoms one site away in the [1̄10] direction, causing features of the two equivalent orientations to be aligned more closely along the [1̄10] direction. Figure 8 is a schematic diagram of the Ni{110} surface with the proposed adsorption sites for thiophene indicated by ovals.

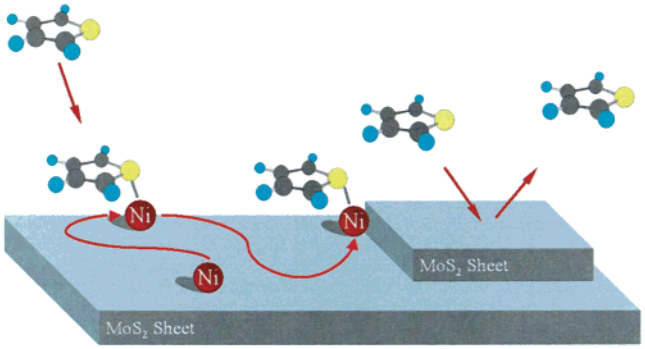

Figure 9. Schematic representation of the proposed mechanism for enhancing the sticking and mobility of reactants. Thiophene molecules impinging on the unreactive basal plane of the MoS_2 surface do not bind to the basal plane surface. However mobile Ni adatoms adsorbed to the MoS_2 basal plane are well suited to form inorganic complexes with the thiophene molecules, thus increasing the effective sticking coefficient of thiophene. These Ni−thiophene complexes can then diffuse around the surface until reaching an active step edge site where hydrodesulfurization can occur.

4. Discussion

We have presented the results of our STM study of Ni atoms and clusters adsorbed on the MoS_2 surface. On MoS_2, Ni atoms are found to be extremely mobile, with rapid diffusion occurring at 77 K and some diffusion and tip-induced mobility apparent at 4 K. Nickel clusters are also observed on the MoS_2 surface; electronic spectroscopy of the clusters shows enhancement of empty electronic states and depletion of filled electronic states relative to the surrounding substrate. This electronic structure would be favorable for binding nucleophilic (electron-donating) species such as thiophene. We have additionally investigated the binding of thiophene to the Ni{110} surface. STM images of thiophene that resolve the underlying Ni{110} lattice indicate that the molecule is bound through the sulfur atom at a 4-fold hollow site.

From our experimental results, detailed above, we hypothesize that Ni species adsorbed on the MoS_2 basal plane bond to the sulfur atoms of thiophenic compounds, creating adsorbed inorganic complexes. These inorganic complexes, due to their expected low barrier to diffusion, are able to diffuse about the surface until reaching active sites at the MoS_2 sheet edges.[59] Figure 9 is a schematic diagram illustrating the mechanism proposed. Thiophene molecules impinging on the bare MoS_2 surface scatter from the surface due to the weak interaction between the surface S atoms and the molecule.[8] This is a result of the saturated bonding of S in the surface plane. Mobile Ni adatoms on the MoS_2 basal plane can bind the thiophene molecules to the near surface region, and the inorganic complex can then diffuse about the surface until reaching a reactive edge site.[60] This proposed mechanism is consistent with EXAFS measurements[61] that have concluded that thiophene is adsorbed initially via the S atom to the promoter. This is consistent with the observation that increased basal plane area leads to higher reactivity even when the number of active sites is held constant. Also, a Ni−thiophene complex diffusing to a MoS_2 edge site would be prealigned in the proper geometry for reaction.

The conditions under which we have studied the behavior of Ni atoms and clusters on MoS_2 are different from those present in "real world" HDS catalysis, and include differences in temperature, sulfidation conditions, and physicochemical state

of the Ni(Co)/MoS_2 catalyst. Certainly, we do not expect that the behavior observed in the current experiment will be exactly reproduced in the reactions taking place during HDS catalysis. However, the mechanism we have proposed (based upon our direct experimental evidence of Ni atom mobility) could well be applicable toward a complete understanding of HDS. Furthermore, our proposed mechanism constitutes a novel aspect of HDS catalysis hitherto unexamined.

Ni promoters on the MoS_2 basal plane will most likely be largely sulfided under the reaction conditions used for HDS.[18] Attachment of atomic S or thiol groups (S−H) to the Ni adatoms will increase the species mobility due to the associated reduction in charge transfer between Ni and the MoS_2 surface. Since S is electrophilic it will compete with the exposed S of the MoS_2 basal plane for the Ni promoters' electron density, thus weakening the Ni−MoS_2 interaction. Thus, the partial sulfidation of Ni, expected under HDS reaction conditions, will act to increase the mobility of the Ni promoters adsorbed on the basal plane. This increased mobility is balanced by attractive interactions that will cause Ni to cluster and to stick to edge sites of the crystallites.

The ability to form Ni−thiophene complexes would effectively increase both the sticking probabilities and the surface mobilities of thiophenes. Without such a mechanism the weak interactions of thiophenes with the MoS_2 basal plane would dictate that only molecules that impact the MoS_2 surface at (or near) sheet edges could react. Salmeron et al.[8] calculated an adsorption energy for thiophene on MoS_2(0001) of 9.5 kcal/mol from their thermal programmed desorption data by performing a Redhead analysis[62] with an assumed preexponential factor of 10^{13} s^{-1}. From this value the adsorption time can be calculated. At a temperature of 350 °C (approximate reaction conditions[13]), thiophene would have a surface residence time of ∼200 ps. Thus, only molecules that landed at or could diffuse to an active step site within this residence time would have the chance to undergo HDS. The formation of stable Ni−thiophene complexes would thus have great impact on the catalytic activity by enabling more reactant molecules to reach the active edge sites.

To gain an understanding of the importance of such a process it is instructive to gauge the relative strength of thiophene bonding to the different species involved. This can be accomplished by investigating the manner in which thiophene adsorbs to bare single-crystal metal surfaces. It has been reported that at low coverage thiophene adsorbs to Mo{100} with its molecular ring parallel to the surface and decomposes in the 100−300 K temperature range.[63] The C−S bond cleavage and decomposition of thiophene upon adsorption on Ni{100} at temperatures as low as 90 K demonstrates the strength of the Ni−S bond.[64] Thus, it can be seen that thiophene binds strongly to both pure Mo and Ni; however, this is not the most common chemical state for these metals during the catalytic reaction. Infrared spectroscopy of thiophene adsorbed on a supported MoS_2 catalyst determined that thiophene bonds through its sulfur atom to coordinately unsaturated (cus) Mo sites.[65] The interaction between the cus Mo site and thiophene is reduced from that of the bare Mo surface—thiophene desorbs intact from the surface at 243 K.[65] Thus, it should be expected that the Ni−thiophene interaction will also be moderated if the Ni atoms/clusters are partially sulfided. However, Ni has a strong affinity for thiophene and thus the inorganic complexes formed should have sufficient stability to allow their diffusion to the active edge sites.

We do expect that the majority of promoter atoms will be tied up at step edge sites known to dominate reactivity.[3,14] Thus, the ability of Ni atoms to detach and transit the basal planes will likely determine the catalytic importance of such a mechanism.[21] From such edge sites and other binding sites for promoters we expect a two-dimensional vapor pressure of promoters on the basal planes. A similar equilibrium between a two-dimensional gas and one-dimensional solid was observed for benzene adsorbed on Cu{111}.[44] Thus, even if the Ni atom that is part of the inorganic complex actively takes part in the HDS reaction once the complex reaches the active site, other promoter atoms will be desorbing onto the basal plane and thus be available to bind more reactant molecules. The chemical forms and cluster sizes of these promoter species will depend on the specific reaction conditions.

Ni(Co) promoter species at the edge sites are believed to be bound to five S atoms.[14−16,66,67] A Ni atom on the MoS_2 basal plane has the ability to bond with three basal plane S atoms (by sitting in a 3-fold hollow site). Thus, a Ni atom would at most have to break two sulfur bonds upon "2D desorption" from the step edge onto the basal plane. However, it seems more likely that a Ni−S or Ni−S−H species would desorb from the edge site. Such a species would only need to break one Ni−S bond and thus should only have a small barrier for desorption onto the MoS_2 basal plane. As discussed above, such sulfided mono-Ni species are expected to be even more mobile than the bare Ni adatoms investigated in our studies. Bonding S (and Cl) atoms to Ni{100} and Cu{100} reduces the bond strength of the bound metal atoms to their neighbors as evidenced by interlayer and intralayer relaxations and increased Debye−Waller factors in SEXAFS measurements.[68] Attaching electronegative species to metal substrates can enhance the mobility of the substrate atoms through motion of substrate−adsorbate complex.[69] In order to calculate the actual barrier for desorption it would be necessary to determine the free energy of the Ni at an edge site and Ni on the basal plane. Although such a calculation has not been performed, stable organometallic analogues of Ni(Co) coordinated to four S species exist, supporting the stability of the proposed Ni−S basal plane species.[70]

Although this type of catalytic mechanism is novel for heterogeneous catalysis, it is not without analogy. The proposed mechanism is quite similar to phase transfer catalysis in two-phase liquid media.[71] A phase transfer catalyst (often a complexing agent such as a crown ether) increases reactivity by shuttling reactants across the interface between aqueous and organic phases. In both mechanisms the transfer agent (in our case Ni adatoms) increases the reactant concentration at the active site, which in turn increases the catalytic activity.

5. Conclusions

We have described low-temperature STM investigations into the dynamics and electronic structures of Ni adsorbed to the basal plane of MoS_2, as well as thiophene adsorption on Ni{110}. From our experimental findings, we propose that in addition to their role in modifying the surface chemistry directly, metal promoters on MoS_2 HDS catalysts (1) bind reactants to unreactive portions of the catalytic surface, and (2) transport reactants to active sites on the anisotropic catalytic surface. These two new roles in conjunction with their conventional electronic and structural effects could more fully explain the function of Ni and Co promoters on MoS_2 HDS catalysts. Experiments are currently underway to demonstrate the concerted diffusion of Ni-thiophene complexes as well as to investigate the geometry of the active edge sites directly.

Acknowledgment. We thank Charlie Campbell, Michel Daage, Ken Riley, Hans-Peter Rust, and Henrik Topsøe for helpful discussions. We thank Gabor Somorjai for his encouragement of this work and congratulate him on his 65th birthday, celebrated with this special issue of *The Journal of Physical Chemistry B*. We gratefully acknowledge the financial support of the National Science Foundation, the Office of Naval Research, Petroleum Research Fund administered by the American Chemical Society, the Exxon Education Foundation, and Air Products. J.G.K. thanks the Braddock Graduate Fellowship for support. P.S.W. thanks the Alfred P. Sloan Foundation and the John Simon Guggenheim Memorial Foundation for fellowship support.

References and Notes

(1) Somorjai, G. A. *Introduction to Surface Chemistry and Catalysis*; John Wiley and Sons: New York, 1994.

(2) E.g.: Gellman, A. J.; Neiman, D.; Somorjai, G. A. *J. Catal.* **1987**, *107*, 92−102. Zaera, F.; Kollin, E. B.; Gland, J. L. *Surf. Sci.* **1987**, *184*, 75−89. de Jong, A. M.; de Beer, V. H. J.; van Veen, J. A. R.; Niemantsverdriet, J. W. *J. Phys. Chem.* **1996**, *100*, 17722−17724. Peterson, S. L.; Schulz, K. H. *Langmuir* **1996**, *12*, 941−945. Friend, C. M.; Chen, D. A. *Polyhedron* **1997**, *16*, 3165−3175.

(3) E.g.: Topsøe, H.; Clausen, B. S.; Topsøe, N.-Y.; Pederson, E. *Ind. Eng. Chem. Fundam.* **1986**, *25*, 25−36. Chianelli, R. R.; Daage, M.; Ledoux, M. J. *Adv. Catal.* **1994**, *40*, 177−232.

(4) E.g.: Angelici, R. J. *Coord. Chem. Rev.* **1990**, *90*, 61−76. Angelici, R. J. *Bull. Soc. Chim. Belg.* **1995**, *104*, 265−282. Vicic, D. A.; Jones, W. D. *J. Am. Chem. Soc.* **1997**, *119*, 10855−10856. Angelici, R. J. *Polyhedron* **1997**, *16*, 3073−3088. Harris, S. *Polyhedron* **1997**, *16*, 3219−3233. Dullaghan, C. A.; Carpenter, G. B.; Sweigart, D. A.; Choi, D. S.; Lee, S. S.; Chung, Y. K. *Organometallics* **1997**, *15*, 5688−5695.

(5) E.g.: Ruette, F.; Valencia, N.; Sánchez-Delgado, R. *J. Am. Chem. Soc.* **1989**, *111*, 40−46. Rodriguez, J. A. *Surf. Sci.* **1992**, *278*, 326−338. Rodriguez, J. A. *J. Phys. Chem. B* **1997**, *101*, 7524−7534. Raybaud, P.; Hafner, J.; Kresse, G.; Toulhoat, H. *Phys. Rev. Lett.* **1998**, *80*, 1481−1484.

(6) Voorhoeve, R. J. H.; Stuiver, J. C. M. *J. Catal.* **1971**, *23*, 228−235. Voorhoeve, R. J. H.; Stuiver, J. C. M. *J. Catal.* **1971**, *23*, 243−252.

(7) The 4,6 disubstituted dibenzothiophenes are the most difficult compounds to desulfurize found in petroleum feedstocks. Their resistance to HDS is most likely a combination of the high stability of the three-ring structure and the steric blocking effect of the species at the 4 and 6 positions.

(8) Salmeron, M.; Somorjai, G. A.; Wold, A.; Chianelli, R. R.; Liang, K. S. *Chem. Phys. Lett.* **1982**, *90*, 105−107.

(9) Farias, M. H.; Gellman, A. J.; Somorjai, G. A.; Wold, A.; Chianelli, R. R.; Liang, K. S. *Chem. Phys. Lett.* **1984**, *140*, 181−196. Kelly, D. G.; Salmeron, M.; Somorjai, G. A. *Surf. Sci.* **1986**, *175*, 465−486. Roberts, J. T.; Friend, C. M. *Surf. Sci.* **1987**, *186*, 201−218. Friend, C. M.; Chen, D. A. *Polyhedron* **1997**, *16*, 3165−3175. Roe, C. L.; Schulz, K. H. *J. Vac. Sci. Technol. A* **1998**, *16*, 1066−1072.

(10) For a review, see: Wiegand, B. C.; Friend, C. M. *Chem. Rev.* **1992**, *92*, 491−504.

(11) Helveg, S.; Lauritsen, J. V.; Laegsgaard, E.; Stensgaard, I.; Nørskov, J. K.; Clausen, B. S.; Topsøe, H.; Besenbacher, F. *Phys. Rev. Lett.* **2000**, *84*, 951−954.

(12) Clark, P. G., Jr.; Friend, C. M. *J. Chem. Phys.*, in press.

(13) Daage, M.; Chianelli, R. R. *J. Catal.* **1994**, *149*, 414−427.

(14) Topsøe, N.-Y.; Topsøe, H. *J. Catal.* **1983**, *84*, 386−401.

(15) Topsøe, H.; Clausen, B. S. *Catal. Rev.-Sci. Eng.* **1984**, *26*, 395−420.

(16) Byskov, L. S.; Hammer, B.; Nørskov, J. K.; Clausen, B. S.; Topsoe, H. *Catal. Lett.* **1997**, *47*, 177−182.

(17) Topsøe, H.; Clausen, B. S.; Topsøe, N.-Y.; Pederson, E. *Ind. Eng. Chem. Fundam.* **1986**, *25*, 25−36.

(18) Prins, R.; De Beer, V. H. J.; Somorjai, G. A. *Catal. Rev.-Sci. Eng.* **1989**, *31*, 1−41.

(19) Harris, S.; Chianelli, R. R. *J. Catal.* **1986**, *98*, 17−31.

(20) De Beer, V. H. J.; Duchet, J. C.; Prins, R. *J. Catal.* **1981**, *72*, 369−372.

(21) Kushmerick, J. G.; Weiss, P. S. *J. Phys. Chem. B* **1998**, *102*, 10094−10097.

(22) Stupian, G. W.; Leung, M. S. *Appl. Phys. Lett.* **1987**, *51*, 1560−1562.

(23) Magonov, S. N.; Whangbo, M. H. *Adv. Mater.* **1994**, *6*, 355−371.

(24) Weimer, M.; Kramer, J.; Bai, C.; Baldeschweiler, J. D. *Phys. Rev. B* **1988**, *37*, 4292−4295.

(25) Sarid, D.; Henson, T. D.; Armstrong, N. R.; Bell, L. S. *Appl. Phys. Lett.* **1988**, *52*, 2252−2254.

(26) Coleman, R. V.; Giambattista, B.; Hansma, P. K.; Johnson, A.; McNairy, W. W.; Slough, C. G. *Adv. Phys.* **1988**, *37*, 559−644.

(27) Tang, S. L.; Kasowski, R. V.; Parkinson, B. A. *Phys. Rev. B* **1989**, *39*, 9987−9991.

(28) Youngquist, M. G.; Baldeschweiler, J. D. *J. Vac. Sci. Technol. B* **1991**, *9*, 1083−1087.

(29) Altibeli, A.; Joachim, C.; Sautet, P. *Surf. Sci.* **1996**, *367*, 209−220.

(30) Whangbo, M.-H.; Ren, J.; Magonov, S. N.; Bengel, H.; Parkinson, B. A.; Suna, A. *Surf. Sci.* **1995**, *326*, 311−326.

(31) Heckl, W. M.; Ohnesorge, F.; Binnig, G.; Specht, M.; Hashmi, M. *J. Vac. Sci. Technol. B* **1991**, *9*, 1072−1078.

(32) Permana, H.; Lee, S. K.; Ng, Y. S. *J. Vac. Sci. Technol. B* **1992**, *10*, 2297−2301.

(33) Chu, X.; Schmidt, L. D. *J. Catal.* **1993**, *144*, 77−92.

(34) Angelici, R. J. *Acc. Chem. Res.* **1988**, *21*, 387−394.

(35) Zaera, F.; Kollin, E. B.; Gland, J. L. *Langmuir* **1987**, *3*, 555−557.

(36) Huntley, D. R.; Mullins, D. R.; Wiegeier, M. P. *J. Phys. Chem.* **1996**, *100*, 19620−19627.

(37) Frank, E. R.; Chen, X. X.; Hamers, R. J. *Surf. Sci.* **1995**, *334*, L709−L714.

(38) Chen, X.; Frank, E. R.; Hamers, R. J. *J. Vac. Sci. Technol. B* **1996**, *14*, 1136−1140.

(39) Ferris, J. H.; Kushmerick, J. G.; Johnson, J. A.; Youngquist, M. G. Y.; Kessinger, R. B.; Kingsbury, H. W.; Weiss, P. S. *Rev. Sci. Inst.* **1998**, *69*, 2691−2695.

(40) Vacuum Generators, Hastings, E. Sussex, England. http://www.vacgen.com/vacgen/vg-home.htm.

(41) The molybdenite samples used were mined in Ontario, Canada, and obtained from Nature's Window, Wyomissing, PA.

(42) Our STM and associated control electronics are optimized for stability and low noise signals. A typical image takes 5 min to acquire.

(43) Binnig, G.; Fuchs, H.; Stoll, E. *Surf. Sci. Lett.* **1986**, *169*, L295−L300.

(44) Stranick, S. J.; Kamna, M. M.; Weiss, P. S. *Science* **1994**, *266*, 99−102.

(45) Stranick, S. J.; Kamna, M. M.; Weiss, P. S. *Surf. Sci.* **1995**, *338*, 41−59.

(46) (a) Eigler, D. M.; Schweizer, E. K. *Nature* **1990**, *344*, 524−526. (b) Zeppenfeld, P.; Lutz, C. P.; Eigler, D. M. *Ultramicroscopy* **1992**, *42−44*, 128−133. (c) Weiss, P. S.; Eigler, D. M. *Nanosources and Manipulation of Atoms Under High Fields and Temperatures: Applications*; Kluwer Academic Publishers: The Netherlands, 1993; pp 213−217.

(47) Bartels, L.; Meyer, G.; Rieder, K.-H. *Phys. Rev. Lett.* **1997**, *79*, 697−700.

(48) Stroscio, J. A.; Feenstra, R. M.; Newns, D. M.; Fein, A. P. *J. Vac. Sci. Technol. A* **1988**, *6*, 499−507.

(49) Papageorgopoulos, C.; Kamaratos, M. *Surf. Sci.* **1985**, *164*, 353−366.

(50) Hosoki, S.; Hosaka, S.; Hasegawa, T. *Appl. Surf. Sci.* **1992**, *60/61*, 643−647.

(51) Weiss, P. S.; Eigler, D. M. *Phys. Rev. Lett.* **1992**, *69*, 2240−2243.

(52) Kamna, M. M.; Stranick, S. J.; Weiss, P. S. *Science* **1996**, *274*, 118−119.

(53) Ruan, L.; Besenbacher, F.; Stensgaard, I.; Lægsgaard, E. *Phys. Rev. Lett.* **1992**, *69*, 3523−3526.

(54) The raw data used for the Fourier analysis was a 100 Å × 100 Å image that ensured a sufficient number of surface atoms to enable a dependable Fourier space image to be formed. The two images were cropped from this larger data set to highlight the two thiophene orientations.

(55) The entire Fourier transform filtering process was performed with *Scion Image* an image processing and analysis program based on *NIH Image* and freely distributed on the World Wide Web (http://www.scioncorp.com).

(56) Buisset, J.; Rust, H.-P.; Schweizer, E. K.; Cramer, L.; Bradshaw, A. M. *Phys. Rev. B* **1996**, *54*, 10373−10376.

(57) Doering, M.; Buisset, J.; Rust, H.-P.; Briner, B. G.; Bradshaw, A. M. *Faraday Discuss.* **1996**, *105*, 163−175.

(58) Doering, M.; Rust, H.-P.; Briner, B. G.; Bradshaw, A. M. *Surf. Sci.* **1998**, *410*, L736−L740.

(59) Stranick, S. J.; Parikh, A. N.; Allara, D. L.; Weiss, P. S. *J. Phys. Chem.* **1994**, *98*, 11136−11142.

(60) Although the promoter−reactant species is shown schematically reaching an active site at the edge of a neighboring MoS_2 sheet, the proposed mechanism also includes the promoter−reactant species reaching an active site at the edge of the MoS_2 sheet on which they are diffusing.

(61) Topsøe, H.; Clausen, B. S.; Topsoe, N.-Y.; Zeuthen, P. In *Catalysis in Petroleum Refining 1989*; Studies in Surface Science and Catalysis, Vol. 53; Trimm, D. L., Akashah, S., Absi-Halabi, M., Bishara, A., Eds.; Elsevier: Amsterdam, 1990; pp 77−102.

(62) Redhead, P. A. *Vacuum* **1963**, *12*, 203−211.

(63) Zaera, F.; Kollin, E. B.; Gland, J. L. *Surf. Sci.* **1987**, *184*, 75−89.

(64) Stohr, J.; Kollin, E. B.; Fischer, D. A.; Hastings, J. B.; Zaera, F.; Sette, F. *Phys. Rev. Lett.* **1985**, *55*, 1468−1471.

(65) Tarbuck, T. L.; McCrea, K. R.; Logan, J. W.; Heiser, L.; Bussell, M. E. *J. Phys. Chem. B* **1998**, *102*, 7845−7857.

(66) Byskov, L. S.; Nørskov, J. K.; Clausen, B. S.; Topsøe, H. *Proc. Pet. Chem.* (*ACS, Div. Pet. Chem.*) **1998**, *43*, 12−14.

(67) E.g.: Topsøe, H.; Massoth, F. E.; Clausen, B. S. Catalytic Hydroprocessing: Catalyst Structure and Chemistry. In *Catalysis, Science and Technology*; J. Anderson, R., M. Boudart, M., Eds.; Springer-Verlag: New York, 1996; Vol. 11.

(68) Sette, F.; Hashizume, T.; Comin, F.; MacDowell, A. A.; Citrin, P. H. *Phys. Rev. Lett.* **1988**, *61*, 1384−1387.

(69) Stranick, S. J.; Parikh, A. N.; Allara, D. L.; Weiss, P. S. *J. Phys. Chem.* **1994**, *98*, 11136−11142.

(70) Holmes, R. R. *Prog. Inorg. Chem.* **1984**, *32*, 119−235.

(71) Gates, B. C. *Catalytic Chemistry*; John Wiley & Sons: New York, 1992.